Microtechnology Department

Head: Gábor BATTISTIG, Ph.D.

Research Staff

Mária ÁDÁM, M.Sc.
István BÁRSONY, D.Sc., scientific advisor, Director of MTA MFA
Ferenc BELEZNAY, D.Sc., Professor Emeritus
Csaba Sándor DARÓCZI, dr. univ.
László DÓZSA, Ph.D.
Csaba DÜCSŐ, Ph.D.
Péter FÜRJES, Ph.D.
Zsolt József HORVÁTH, Ph.D.
Albert KARACS, M.Sc.
Zoltán LÁBADI, Ph.D.
György MOLNÁR, Ph.D.
Ákos NEMCSICS, Ph.D. (part time)
Andrea Edit PAP, Ph.D.
István PINTÉR, Ph.D.
Vilmos RAKOVICS, Ph.D.
Vo Van TUYEN, Ph.D., (on leave)
Gábor VÁSÁRHELYI, Ph.D.
Éva VÁZSONYI, M.Sc.
Zsolt ZOLNAI, Ph.D.

Ph.D. students / Diploma workers

Péter BASA, Ph.D. student
Edvárd Bálint KUTHI, Ph.D. student (on leave)
Ágoston NÉMETH, Ph.D. student
Anita PONGRÁCZ, Ph.D. student

Technical Staff

György ALTMANN, technician
Edvárd BADALJÁN, engineer
Tamás BERKÓ, engineer
Sándor CSARNAI, technician
Ábel DEBRECZENY, technician
Magdolna ERŐS, technician
Csilla FARAGÓ, technician
János FERENCZ, technician
Alajos GONDOS, technician
Tamás JÁSZI, technician (on leave)
Viktor KULIN, engineer
Csaba LÁZÁR, engineer
György LEHEL, technician
Ákos MAJOROS, engineer
Attila NAGY, technician
Sándor PÜSPÖKI, engineer (part time)
Sándorné PÜSPÖKI, engineer
István RÉTI, engineer
Imre SZABÓ, engineer
Tamás SZABÓ, engineer
Magdolna VARGA, technician
Katalin VERESNÉ VÖRÖS, engineer
József WAIZINGER, engineer

Main Activities

Research and development of physical, chemical/biochemical sensors and integrated systems:

- MEMS and MEMS related technology, with special emphasis on development of Si MOS embedding circuits.
- Development and applications of near IR light emitting diodes and detectors.
- Solar cells and their competitive technology.
- Acoustic wave devices and their application.

Fundamental research on:

- sensing principles
- novel materials and nanostructures
- novel 3D fabrication techniques
- ion-solid interaction for supporting MEMS development.

Device and material characterization.

Facilities

- 300 m^2 clean room (class 10 - 10000) with complete Si wafer processing line. Actually set for 3 and 4 inch diameter. See the Figures 1(a) - 1(h) below.
- 50 m^2 mask laboratory (class 100) for chromium masks up to 5 inch, Fig. 1(i).
- Mask processing with resolution of 1 μm.
- Alkaline and porous Si bulk micromachining.
- Mounting and encapsulation.
- Device testing and electrical characterization.

(a)

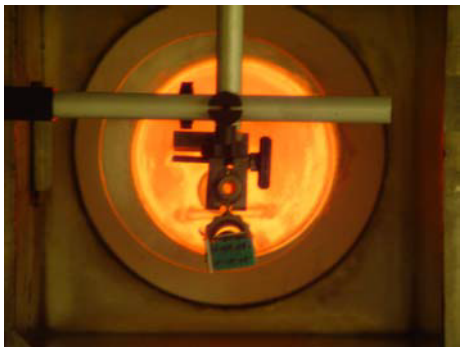

(b)

Figure 1

(c)

(d)

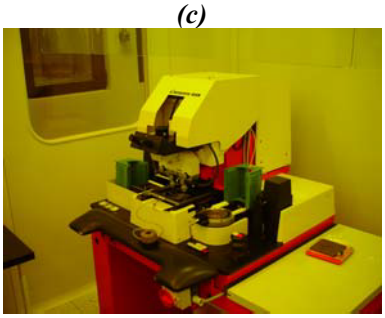

(e)

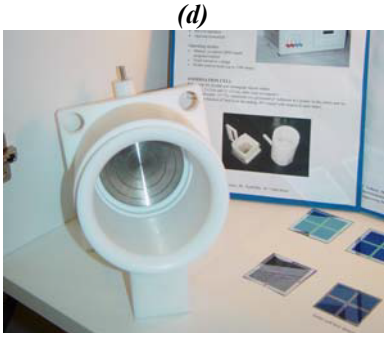

(f)

(g)

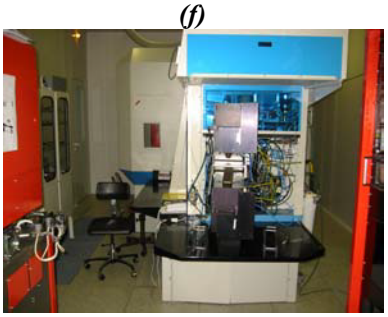

(h)

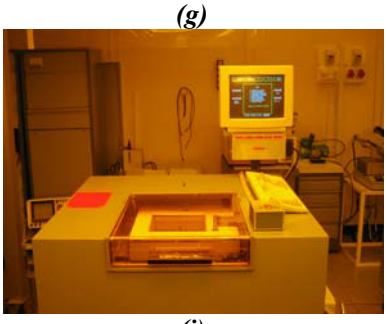

(i)

Figure 1 *continuation*

Production

Calorimetric gas sensors with microfilament structure – Figs. 2(a), (b), and sensitive coatings – Figs. 2(c), (e), custom design and packaging – Figs. 2(d), (f); the hotplate dimensions: 100×100×1 μm^3

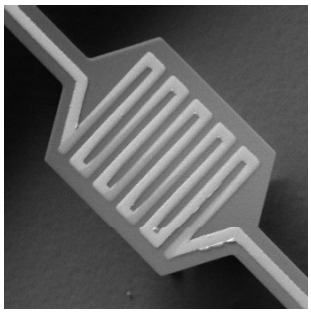

(a)

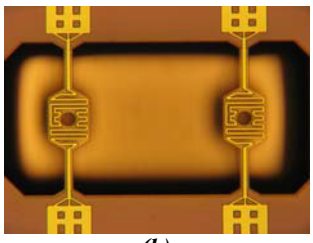

(b)

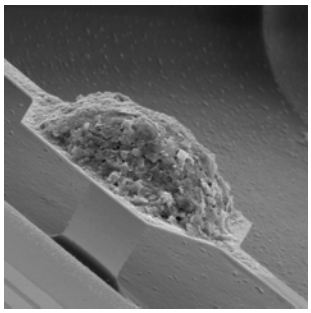

(c)

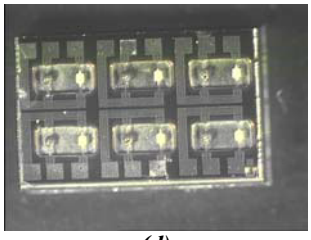

(d)

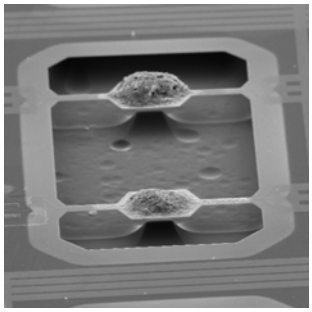

(e)

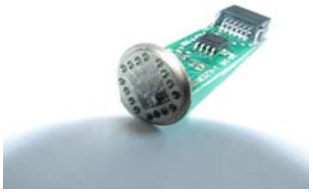

(f)

Figure 2

Development, custom design and small scale production of Si piezoresistive and capacitive pressure sensors – Fig. 3(a) and SAW filters – Fig. 3(b) (center frequency 10-250MHz).

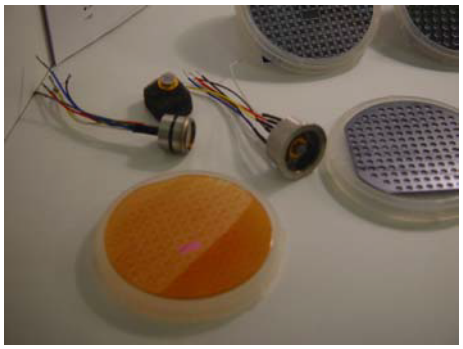

(a)

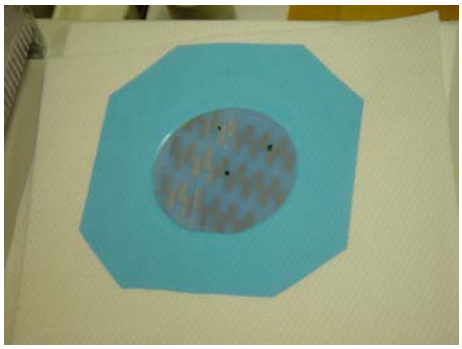

(b)

Figure 3

Development and small scale production of tactile sensor and sensor array fabricated by piezoresistive bulk micromachining technology: TactoPad is the 8×8 three-axial taxels array Fig. 4(c), and (d), the layout design – Fig. 4(a) and the packed device – Fig. 4(b). TactoFlex 2×2 is a small three-axial sensor array – Fig. 4(e) on a flexible support, designed for finger-mounted application – see Fig. 4(f). A spin-off company, **TactoLogic** (www.tactologic.com) has been launched for the further development and for the commercialization of the tactile sensors.

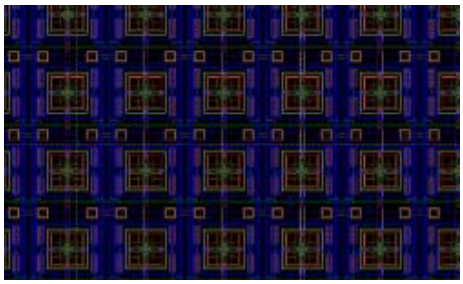

(a)

(b)

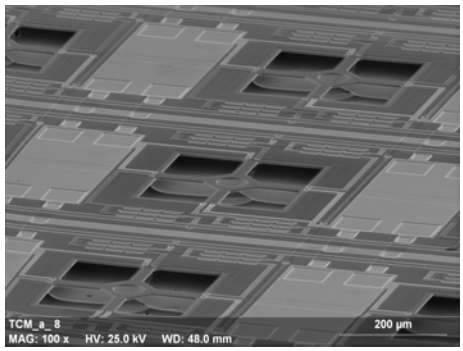

(c)

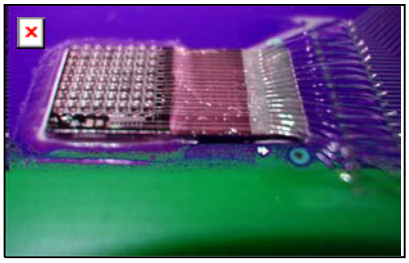

(d)

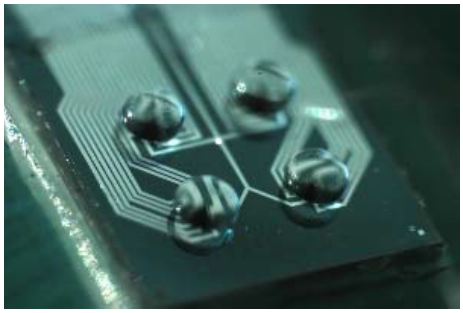

(e)

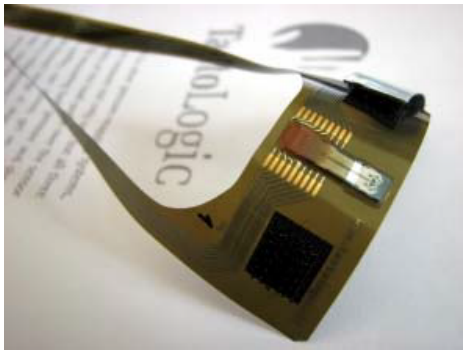

(f)

Figure 4

Fundamental research on:

- sensing principles
- novel materials and nanostructures, cantilever and bridge structures, Si and dielectric membranes
- novel 3D fabrication techniques – porous Si based Si micromachining, see Fig. 5(a), (b), (c), and (d) below.
- ion-solid interaction for supporting MEMS development.

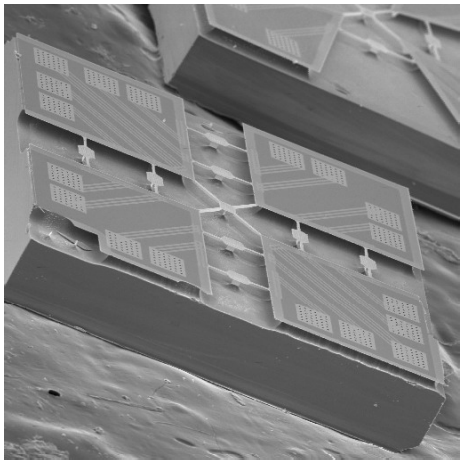

(a)

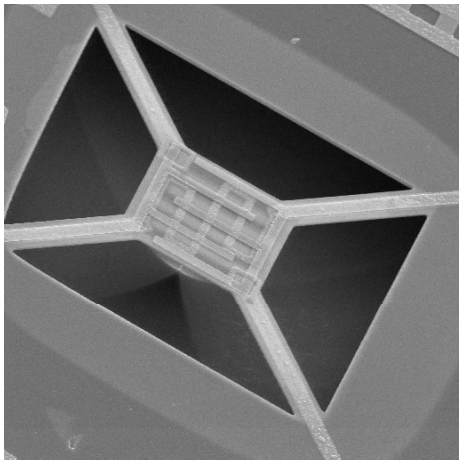

(b)

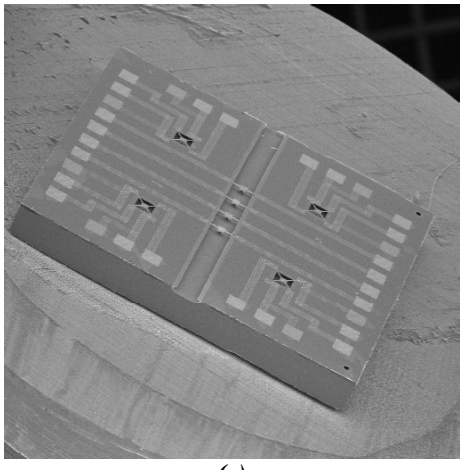

(c)

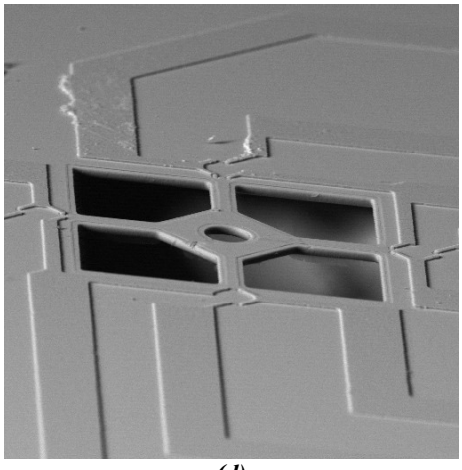

(d)

Figure 5

Design and realization of cantilever microphones for photo-acoustic gas detector system

(NKFP3-00021/2005 project, "Development and Field Application of Complex Photoacoustic Systems for Monitoring Environmental Conditions", 2005-2008)

P. Fürjes, Cs. Dücső

An extremely sensitive photo-acoustic gas detector system is developed to analyse the methane circulation of living forests. The method is based on the detection of the pressure wave generated by the selective energy absorption of the interested gas component which is excited by an adequate laser-pulse in the test chamber. The MFA was working to realize a micro cantilever microphone which is capable to detect the methane gas content in the ppm range through the deformation of the suspended reflective micro-membranes. The circumspect geometric and materials design of the suspending multilayer microstructures is a crucial object of the research.

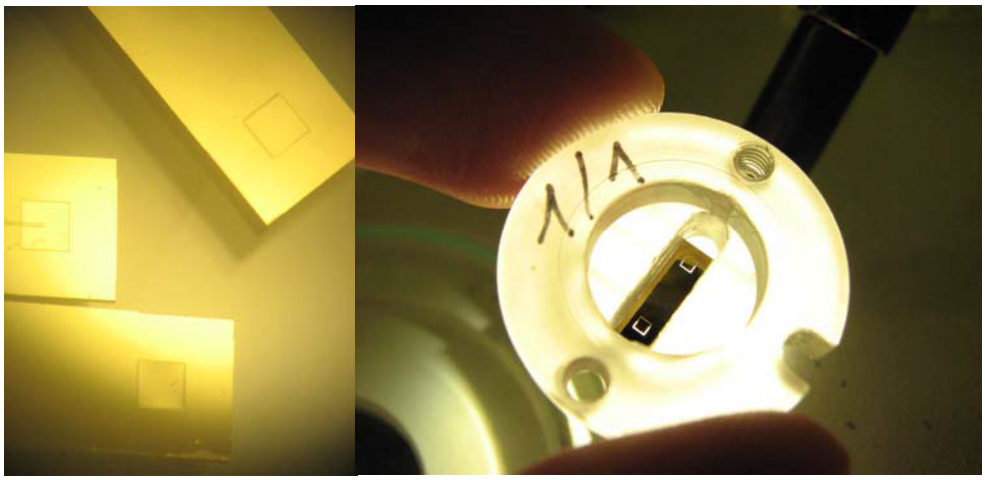

Figure 6 *The manufactured micro-cantilever structures (left) and a packaged device (right).*

3D MEMS structures including two optical microphones were designed, developed, and manufactured applying reliable realization technology, fitting these structures to the active and reference flow chambers of the opto-acoustic measuring system. The adequate structures were manufactured by two side bulk micromachining silicon technology achieving remarkable improvement of the former membrane formation techniques. For the formation of these structured thin layers (reflective membranes suspended by flexible arms) which forms the moving part of the sensor structure, a special structuring process has been developed combining the selective lateral doping with Electrochemical Etch Stop and Reactive Ion Etching processes. The

ElectroChemical Etch Stop process was significantly improved using the anisotropic alkaline etching to form 2-4 μm thick compact silicon membranes applying the ProTEK polymer (Brewer Science) for selective protection of the active area of the sensor structure.

Si MEMS by Proton Beam Writing and porous Silicon micromachining

(Hungarian Scientific Research Fund under Grant No. T O47002)

Cs. Dücső, P. Fürjes, I. Rajta

3D microfluidic Si devices characterized by vertical walls of high aspect ratio were formed by combination of proton beam writing (PBW) technique and subsequent selective porous Si (PS) etching. Crystal damage generated by the implanted protons results in increased resistivity, that limits or even cease the current flow through the implanted area during electrochemical etching. Characteristic feature of the proposed process is that the shape of the MEMS components are defined by two implantation energies, i.e. higher energy is applied to define the frame of the device while lower energy is used to write the moving components. The implantation energies were selected such as to result appropriate difference between the two projection ranges, taking into consideration the thickness of the walls of the moving component and the isotropic etching profile of the electrochemical PS formation. The electrochemical etching is stopped when the sacrificial PS layer completely underetches the moving components but the etching front does not yet reach the bottom of the frame. Therefore, the dissolution of PS results in a ready-to-operation device with a released moving component embedded. The feasibility of the process is demonstrated by the fabrication of micro turbines and non return valves.

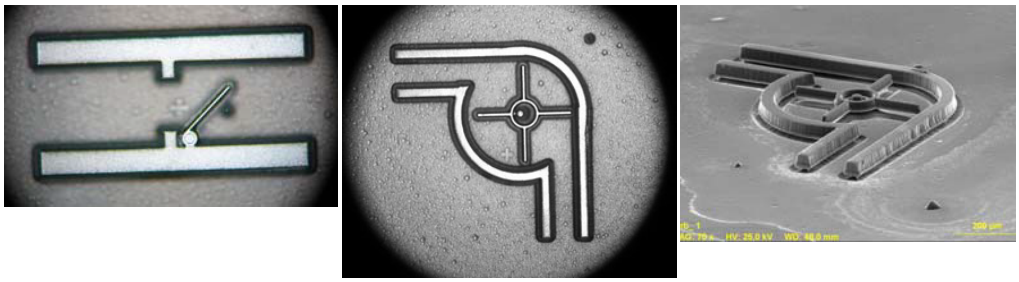

Figure 7 *Microfluidic valve (left) and turbine (middle & right) realized by proton direct writing and porous Si etching*

Fluidic applications for corrosive environments

P Fürjes, Cs. Dücső, P. Csíkvári

Protective coating of microsystems used in harsh environment is essential for reliable device operation. Due to their well-known superior chemical and abrasion resistance, deposited diamond or diamond like carbon (DLC) layers are among the most attractive candidates for this purpose, providing that the layers prove pinhole-free in the given environment.

In present work we describe and characterize micro-hotplate structures formed by front side porous silicon micromachining process in combination with a three-step multilayer deposition (diamond/polycrystalline-Si/diamond), doping and appropriate patterning. The material of the filament is preferably polycrystalline silicon, however, Pt can also be considered. Selective area deposition (SAD) technique allows patterning of the diamond layers. Although the extremely high thermal conductivity of the deposited polycrystalline diamond layers (260 – 900 W/mK) does not favour the addressed task, our preliminary calculations show that temperature of 100^{o}C can be reached by less than 100 mW input power on the surface of the two-arm suspended hotplate. Beside the thermal and thermo-mechanical properties of the hotplates, the chemo-protective effect of the diamond layer was investigated.

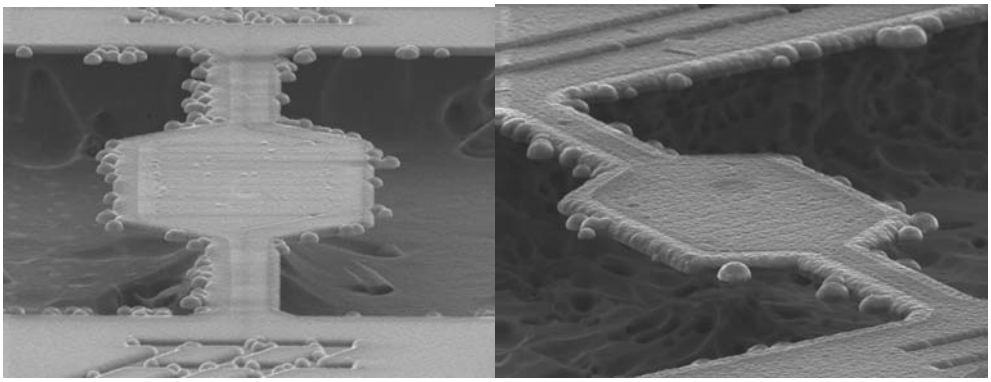

Figure 8 *Poly-silicon micro-heater formed by diamond SAD technique.*

Investigation of actuation phenomena and controllable moving microstructures

(Hungarian Scientific Research Fund under Grant No. F 61583)

P. Fürjes

The research of the realization and application of controllable moving microstructures was started at the MEMS Laboratory of MFA near the development of sensor

structures. The practicability of the actuation phenomena (electrostatic, magnetic, thermal) and prognosticable functional parameters of the designed structures (deformation, driving frequency, residual stresses of the layer structures) were analyzed by Finite Element Modeling. Test structures were manufactured by the development and application of adequate MEMS techniques, and they were analyzed considering the functional aspects.

Thermo-mechanical analysis of functional layers in MEMS structures

P. Fürjes

Micro-hotplates are basic components of sensors and lab on a chip devices, e.g. as sensors of calorimetric principle, or heaters in chemical micro-reactors. The most frequently used structural materials are silicon-nitride, non-stoichiometric silicon-nitride, silicon-oxinitride, silicon-dioxide and multilayered combination of these materials. Beyond the frequently applied structural materials, protective coating of MEMS elements used in harsh environment is essential for their reliable operation. The best candidates for such application are diamond, diamond-like-carbon (DLC) or SiC because of their superior chemical and abrasion resistance in aggressive chemicals.

In the micro-hotplate design the most important parameters to be considered are the thermal conductivity, the thermal capacitance and the residual stress in the applied layers in order to select the optimum functionality of the device. While appropriate data are available for the widely used materials (SiO_2, Si_3N_4) this is far not being the case for the non-stoichiometric materials or deposited diamond and DLC layers. Their properties are process dependent, i.e. both their composition and structure are determined by the given individual process. Therefore, relatively simple methods for determination of thermo-mechanical properties are essential in functional design.

We describe alternative techniques for the formation of micro-filaments encapsulated in CVD non-stoichiometric silicon-nitride or multi-crystalline CVD diamond layers and present how the thermal properties of the structural materials can be determined by measuring static and dynamic temperature responses of the micro-hotplate.

Fabrication of SiC nanocrystalline structures

A. Pongrácz, Z. Zolnai, G. Battistig

Epitaxial SiC nanocrystals at the Si side of SiO_2/Si interface made by reactive annealing in CO may be used as templates for heteroepitaxial growth of polycrystalline or even for single crystal SiC layers. We have shown that on Si substrate covered with SiC nanocrystals polycrystalline 3C-SiC layer can be formed without wormholes (Fig. 9) .

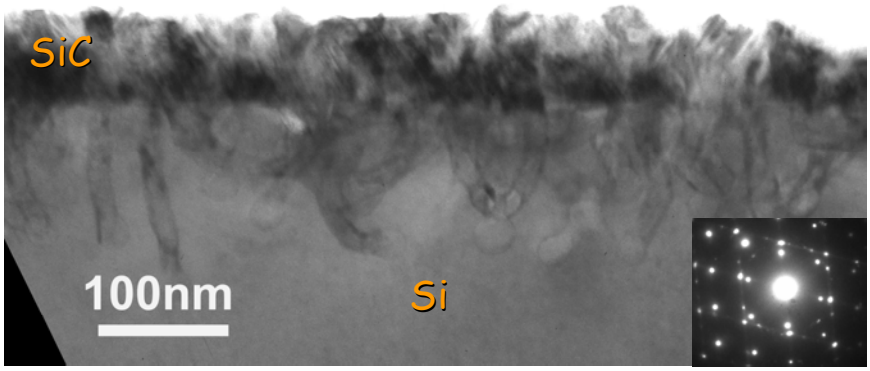

(a)

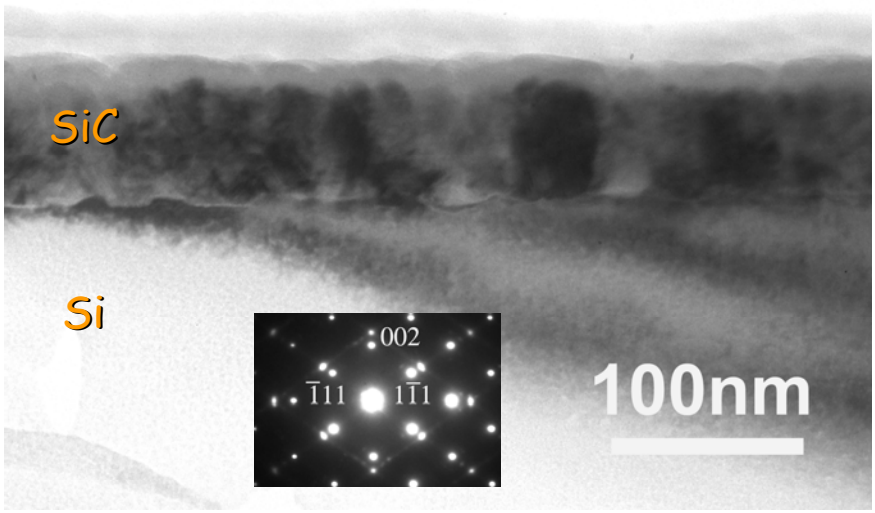

(b)

Figure 9 *Cross sectional transmission electron microscopy image of CVD deposited 3C-SiC layers on (100) Si, (a) conventional method with carbonization step, wormholes are formed during the CVD deposition, (b) SiC nanocrystals formed by CO reactive annealing were used before the CVD step, no void or wormhole formation is present.*

As part of an academic research exchange program Zsolt Zolnai took part in the characterization of 3C-SiC layers made by CVD on Si substrates and Ge(Ga)/Ge(As), GaAs/Ge(As) layers made by MOCVD. New sample set was fabricated for a systematic structure and composition measurement. The characterization methods: XRD, TEM, RBS/C (MFA, Budapest), SIMS/SNMS (ATOMKI, Elektronspectroscopy Department, Debrecen, partners: K. Vad, Z. Berényi, G. Katona). Optimization of growth parameters and growth of epitaxial SiC layers for micromechanical systems, investigation of As diffusion in Ga layers are the main goals of this cooperation.

Fabrication of radiation hard resistive bolometer for ITER

(Contract work for Max Planck Institut für Plasmaphysik)

M. Ádám, É. Vázsonyi, Cs. Dücső

Our goal was the reproduction of a radiation hard resistive bolometer, which is reliable in an environment with high neutron fluxes expected in ITER. Following device specifications made the technology development challenging: ±1,5% resistivity variation of Pt calorimeters on SiN_x membrane, 4-10µm thick W absorber on the backside of the membrane. The most critical part is the sputtering of the thick tungsten absorber layer. Structures have been delivered but we are still developing our technology to reduce the residual stress in the tungsten layer and to control the size of the sputtered area.

Physics and Technology of Elemental, Alloy and Compound Semiconductor Nanocrystals

(EU FP6 project SEMINANO No. 505285, and Hungarian Scientific Research Fund under Grant No. T048696)

Zs. J. Horváth, M. Ádám, J. Balázs, P. Basa, L. Dobos, L. Dózsa, T. Lohner, G. Molnár, P. Petrik, B. Pődör, P. Szöllősi, Z. Zolnai

Semiconductor nanocrystals (NCs) embedded in insulators are usually studied for light emitting and memory purposes. In our group this activity is aimed mainly for memory applications and has been connected with two projects, namely the "Physics and Technology of Elemental, Alloy and Compound Semiconductor Nanocrystals - Materials and Devices" (SEMINANO) EU FP6 project No. 505285 and the "Nanodots and nanolayers in semiconductor structures - electrical and photoelectrical properties" Hungarian Scientific Research Fund (OTKA) under Grant No. T048696.

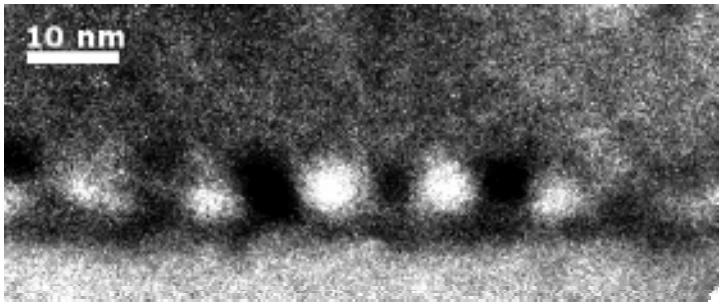

Figure 10 *Energy-filtered XTEM image of sample No. 1 with white dots corresponding to silicon atoms – spherical objects in the middle of the figure are corresponding to the Si NCs embedded between two Si_3N_4 layers.*

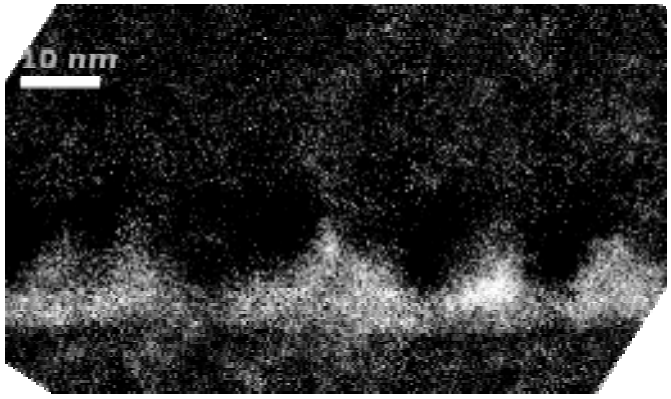

Figure 11 *Energy-filtered XTEM image of sample No. 2 with white dots corresponding to oxygen atoms – image indicates SiO2 pyramids between the Si NCs.*

$Si/SiO_2/Si_3N_4/Si$ NC/Si_3N_4 (No. 1) and $Si/SiO_2/Si_3N_4/Si$ NC/SiO_2/Si_3N_4 (No. 2) multilayer structures with embedded Si NCs were formed, the SiO_2 layers were grown by chemical oxidation of silicon by nitric acid. These samples exhibited good charge injection properties: charging voltage pulses with ±8 V, ±10 V, ±12 V and ±15 V amplitudes and 10 ms width yielded 7.8 V, 10.3 V, 13.1 V and 16.5 V wide memory window width (flat-band voltage difference between the "written" and "erased" state). The extrapolated memory window width for 10 years were expected to be 0.3 V after charge injection with ±12 V, 10 ms pulses. These structures are useful for those applications where small writing/erasing voltage pulse amplitudes are needed, but where information storage for several years is not a requirement.

Optical, electrical and memory properties of MIS structures containing sputtered SiO_x or Al_2O_3 layers with embedded CdSe NCs were characterized in the frame of co-operation with University of Minho, Portugal. Some of the samples exhibited good charge injection properties, yielding the first known observation of such phenomena with CdSe NCs.

Pulsed laser annealing of implantation-amorphized SiC layers

(József Öveges Research Program Under Grant No. SiC_impl.)

Z. Zolnai, A. Karacs, J. Balázs, A. L. Tóth

Nowadays the investigation of single crystalline silicon carbide (SiC) as a candidate for high power, high frequency device industry is an intensive research area. Nevertheless, in this case the problem of selective doping can be solved only by ion implantation. The post-implantation annealing of irradiation-induced lattice damage using either furnace or pulsed laser treatment is not yet solved, however, this obstacle should be overcomed before SiC is applied in semiconductor processing. The aim of this project is to investigate the effect of pulsed laser annealing on both (0001) and (11-20) oriented SiC wafers after ion implantation. On the double side polished (0001) cutted wafers the experiments were done for both front side and back side illumination. The damaged (amorphized) surface SiC layers were produced by Ar^+, P^+, and Ni^+ implantation and the annealing was performed with a Q-switched pulsed Nd:YAG laser operating at wavelengths of λ=1064, 532, and 355 nm.

The single crystal, as-implanted, and post-implantation annealed samples were investigated by Rutherford Backscattering Spectrometry combined with Channeling technique (RBS/C) and with Scanning Electron Microscopy combined with Energy Dispersive X-ray Spectroscopy (SEM/EDS). As the RBS/C results in Fig. 12 show during pulsed laser treatment the annealing and diffusion of crystal defects occurs at the crystalline/amorphous interface of the implanted SiC sample, therefore recrystallization process starts from the bulk side. The significant difference in the SEM/EDX spectra confirms the oxydation of the implanted surface during laser beam annealing which process can stop recrystallization close to the sample surface.

Optical transmission measurements were performed on the implantation-damaged samples, post-annealed by laser pulses with different wavelegths of light and at different geometrical arrangements, i.e. front side or back side (through the transparent substrate) illumination. The measurements were performed to see the changes vs. wavelength in the visible region λ= 360-700 nm, i.e. mainly for below bandgap excitation. As Fig. 12 shows the transparency of the single crystalline SiC sample reduces a lot after implantation. For the as-implanted stage the degree of transmission at λ= 355 nm and λ= 532 nm is similar and the wavelength dependence is weak. This feature is due to the presence of crystal damage and the distortion of the band structure. The annealing process leads to the increase in intensity transfer by reducing the thickness of the amorphous layer and by annihilating the defects. The difference in transparency between unimplanted virgin (v) and post-implantation annealed samples is more significant for wavelengths close to the edge of the bandgap. For pulsed laser annealing at λ= 532 nm the absorption of the sample decreases step by step during the subsequent laser pulses. Consequently, the structural and optical changes due to the annealing process may be saturated for high number of pulses. The similarity in the end stages after several hundreds of laser pulses shown in Fig. 13 can be explained by this saturation phenomena.

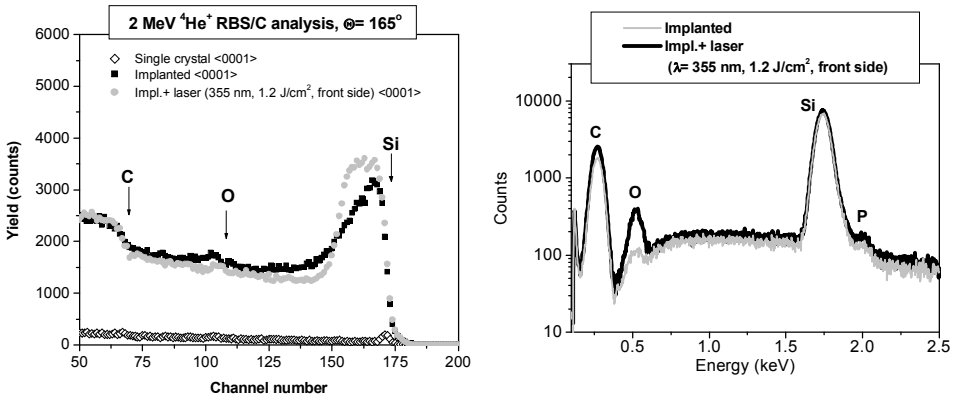

Figure 12 *To the left: The effect of front side pulsed laser annealing on (0001) 4H-SiC amorphized with 120 keV P^+ ion implantation (fluence: 5×10^{15} cm^{-2}) Results of RBS/C measurements, To the right: Energy dispersive X-ray spectrometry (EDX) spectra of the implanted unannealed and the implanted and pulsed laser annealed sample. Parameters of the laser treatment: λ= 355 nm, pulse energy density: J= 1.2 J/cm^2, pulse duration: t= 5 ns ,number of pulses: 200, respectively.*

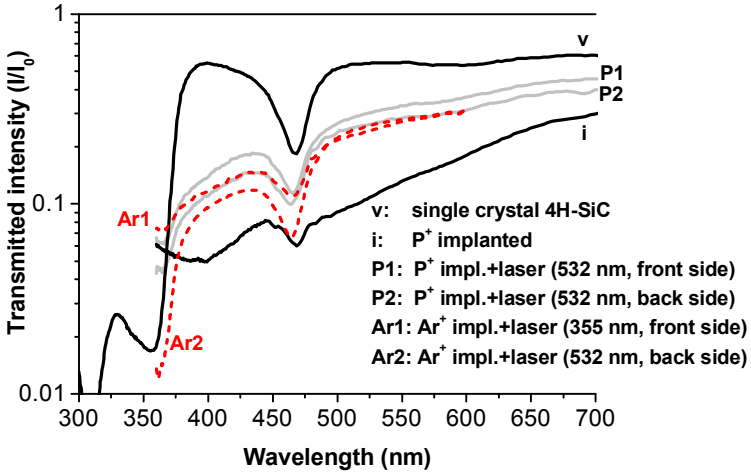

Figure 13 *Optical transmission measured on double side polished 4H-SiC samples with thickness of 400 μm. Data for single crystalline, as-implanted, and post-implantation laser annealed samples are also shown.*

Design of MEMS tactile sensors and their measurement setup

(Joint development with TactoLogic Ltd.)

M. Ádám, I. Bársony, Cs. Dücső, T. Mohácsy, G. Vásárhelyi, É. Vázsonyi

Although the ”Telesense” Sensing Computers and Telepresence Project, granted by the Széchenyi-NKFP has formally ended in 2004, we continued this work with the aim of developing integrated tactile sensor arrays, capable of measuring pressure and force maps. Our sensory unit is a three-dimensional micro force meter. In each array many of these sensors are arranged on a surface. Previously, we have had developed and functionally tested the first smart sensor of the institute: a 64 element three-axial force sensor array, in which we demonstrated – first time worldwide – that the sensors produced by front side porous Si etching can be integrated into standard CMOS circuits in a monolith form. On the prototype chip the MEMS sensors are neighbored by an n-well CMOS decoder, a current generator made of p-channel transistors and transfer gate switches. We also have patents pending on our novel technology.

We integrate this and other similar sensor arrays into evaluation kits for educational and research purposes through a spin-off company founded together with PPKE and SZTAKI. The two other institutes developed the HW and SW parts of the whole sensory system.

This year’s results can be divided into two main parts. On the scientific front the only real advance is a new Ph.D. degree for Gábor Vásárhelyi. On the commercial front we founded our spin-off, TactoLogic Ltd., where Gábor Vásárhelyi (CTO) coordinates the development and system level integration or the tactile sensors. The main results are the following:

- Coordinator work that integrates the product development from the first steps of the MEMS technology through the design of the read-out circuitry to the final design issues
- Final design and product development of the 2×2 tactile chips (TactoPad 2×2 and TactoFlex 2×2)
- Development of 8x8 chips (TactoPad 8×8), connecting the design and the technology
- Integration of the sensor arrays with the read-out device (MasterBoard), design of the communication protocol, connectors, etc.
- Software development with detailed documentation for the first products
- Final design issues of the first real products, including logos, vignettes, connectors, covers, outlook, etc.
- Home page development
- Detailed measurements for qualifying the sensors and their parameters
- General documentation for the products (User’s Manual, Sensor DataSheets, Software Guide, Installation Notes)
- Ads, leaflets, posters, pictures, demo videos, etc.

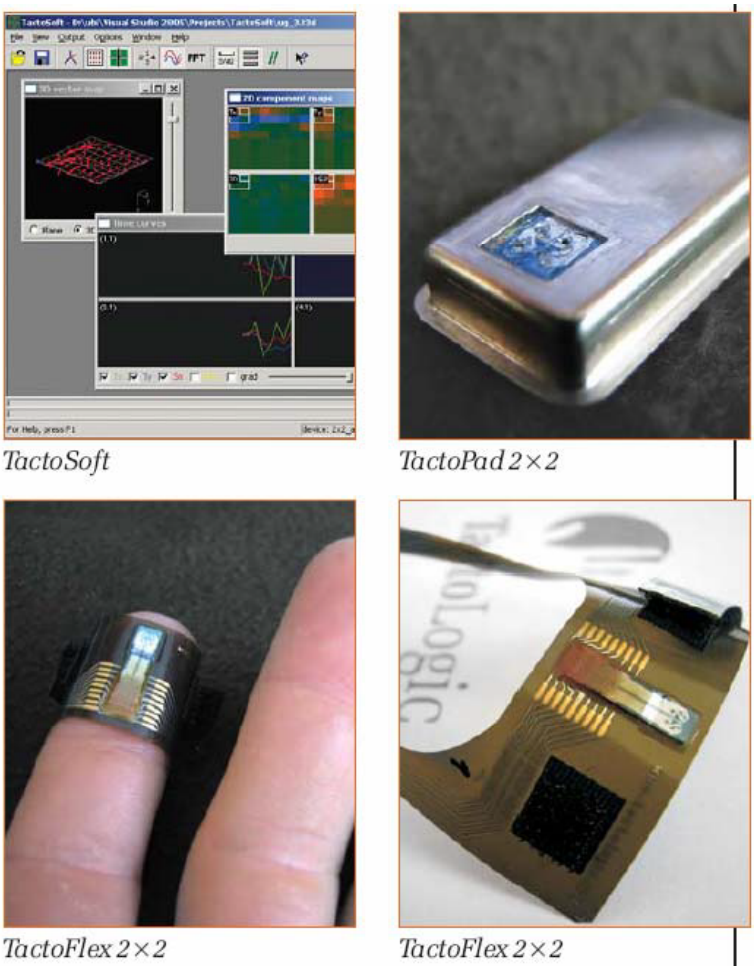

Figure 14
Product versions of the 2×2 (4) element tactile chip

The development of indoor solar cells

B. Szentpáli, I. Pintér, E. Kuthi, Cs. Dücső, M. Ádám, Z. Lábadi, Á. Németh, V. Rakovics, T. Mohácsy

In the course of cooperation with Tateyama Kagaku Ltd. the coworkers of our department developed a single crystal Silicon indoor solar cell with shallow emitter made by plasma immersion ion implantation (PIII). Optimizing the heat treatment of the screen printed contacting paste we were able to make good contacts to shallow PIII emitters of the solar cells that were intended for indoor environment.

The efficiency of indoor solar cells was recorded at four different mixed illumination circumstances. Two different solar light illuminations were applied (one measured indoor in the room with light scattered from the wall in front of the window, while the other light was 1% AM1.5 solar light). These light sources were mixed with indoor fluorescent light of 150 lx, and 700 lx intensity.

The efficiency of the reference a-Si solar cell (made in Japan) is slowly increasing up to 600 lx light intensity, but beyond this intensity the efficiency is gradually decreasing. The efficiency of this cell, however, remains higher than the newly developed c-Si PIII cells up to 1000 lx.

Using fluorescent light at very high illumination, however, the PIII cells have higher efficiency than that of the reference a-Si cell. Even higher is the difference at the advance of PIII cells at mixed illumination measured not far from the window of the room.

We produced ultra shallow emitters for PIII solar cells using low temperature diffusion process. The purpose of this work was to achieve blue sensitivity as high as possible. These cells have efficiencies in the range of 11-13 % at 700 lx indoor fluorescent light.

Figure 15 *The photograph of ultra shallow emitter solar cells with different metallization grids on 5×5 cm^2 Si wafer. In order to obtain optimal serial resistance for the PIII cells, 4 different metal grids were tested. These metal grids are applicable in a wide range of emitter resistance (90-300 Ohm/sq).*

Output power saturation in InGaAsP/InP surface emitting LEDs

V. Rakovics, S. Püspöki, I. Réti

InGaAsP/InP LED's are widely used for optical telecommunication, and for selective spectroscopy in the near infrared range. Observations regarding the temperature sensitivity and power saturation of InGaAsP lasers and light emitting diodes (LED's) have led to extensive studies to find the responsible mechanisms. At high current densities the efficiencies of the diodes drop quickly. The light-current curves are not linear even in short pulse operation.

We prepared and investigated nine different wavelength InGaAsP/InP surface emitting double heterostructure LEDs. Optical power and spectral characteristics of the diodes were investigated as a function of driving current and case temperature. At fixed emitting wavelength, the maximum power is proportional to the volume of the active layer. Short wavelength diodes perform better at high current densities. The output power saturation (Fig. 16) and the temperature sensitivity of the diodes depend on the composition of the active layer.

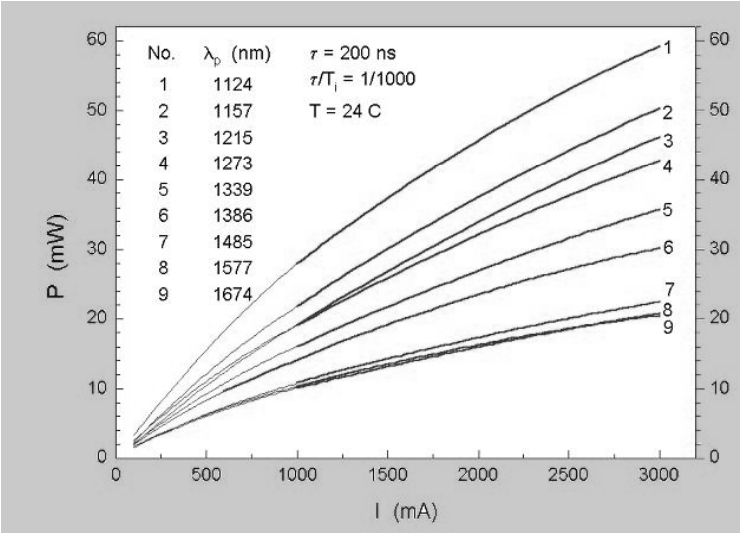

Figure 16 *Output power of the different wavelength LED's as a function of pulse current*

E-field probe for closed space EMC measurements

(GVOP-3.1.1.-2004-05-0354/3.0.)

B. Szentpáli, I. Réti, F. B. Molnár, J. Farkasvölgyi, K. Kazi, Z. Mirk, A. Sonkoly, and Z. Horváth

The generation and measurement of defined electromagnetic fields for radiated immunity test on open area test site is rather expensive. Further the environmental, meteorological conditions strongly influence the measurements. Therefore there is a real need for performing the investigations in closed measuring chambers built in laboratory rooms. Different methods have been proposed in the literature as anechoic chambers, reverberation boxes or TEM cells. In all cases there is a chance for the resonance in the chamber and/or the appearance of spurious modes and therefore the exposed electric field can differ from the expected one. The purpose of this project was the development of an E-field probe for the independent control of the actual value of the microwave field. The probe is an accessory of the measuring chamber, it is connected by a long flexible cable therefore can be placed to a large variety devices under test. It is important that the probe and its cable should not disturb significantly

the field distribution; the sensitivity of the probe should be isotropic, because the test is made at all degrees of polarization.

The traditional isotropic E-field probe construction, with three mutually orthogonal short dipole antenna was applied. The detector diodes are mounted in the gap of the dipoles. The connections between the sensors and the amplifier are 2 m long flexible resistive transmission lines fabricated by screen printing from resistive carbon paste on 0,125 mm thick polyester foil. There is a low-pass filter between the diode and the resistive line. The other end of the resistive line is mounted in a DS type connector; it fits into the socket mounted on the inner wall of the measuring chamber. Facing to it on the outer wall of the chamber there is the equivalent socket for the amplifier.

The effect of the resistive transmission lines on the field distribution were checked first in the GTEM cell. A monopole antenna was fabricated from a semi-rigid cable by removing the outer conductor at the 12 mm long end part. This antenna was fixed in the GTEM cell and the transmission was measured and saved between the feed point of the cell and this antenna in the case when the cell was empty. Then the resistive transmission line was placed into the GTEM cell and the transmission measurement was performed again. The difference of the first and the second transmission spectra was registered. The measurements were made by placing the sensing monopole in 5 measuring points within a 0.5 x 0.5 m^2 square and orienting it to 3 mutually orthogonal directions in each measuring position (IEC 61000-4-20) Fig. 17 shows the measuring set-up. Beyond the field scattering effect of the resistive transmission lines the same investigatins were performed for objects used for fixing, holding the equipments under test. These objects are made from plexiglass, polystyrene foam, wood, etc.

Figure 17 *The measuring set-up for the field scattering effect. In the photo the field distribution of the plexiglass sheet is investigated in the GTEM cell.*

The conclusion of the numerous investigations was that the difference in the transmission was always less than 1 dB in the case of the resistive lines, even when they were arranged very different ways. On the other hand any other conductive wires, or coaxial cables resulted in significantly greater effects, at least at one frequency the difference exceed the 6 dB. It happened also in the case of the thinnest available coaxial cable having only an outer diameter of 1.8 mm. Objects having not too long dimensions, as small metal boxes or coaxial adapters, etc. showed also small

effect on the field, except when they were placed in the immediate vicinity of the monopole.

The resistive line is a low pass filter. The cut-off frequency is about 800 Hz. This is the reason for the application of the simple envelop detector only, having direct DC output. This is the price for the not disturbing character of the probe.

Figure 18 *The calibration of the probe in anechoic chamber with the calibrated horn antenna.*

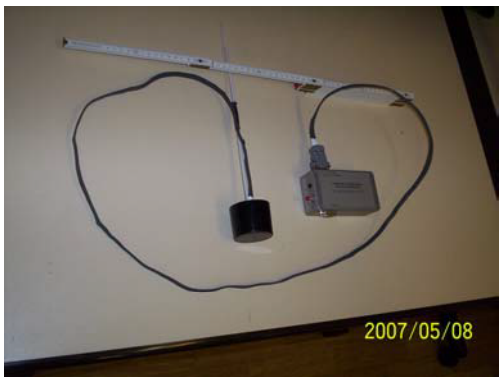

Figure 19 *The isotropic E-field probe with the flexible leads.*

The sensitivity of the probe was calibrated in free space in an anechoic chamber with the help of calibrated antennas. The calibration set-up is shown in Fig. 18.

The DC output voltage of the individual sensor is amplified and digitalised with a resolution of 12 bit. The bit values of the voltage (LSBs) are feed to a personal computer via the serial port. The measured data are shown in real time on the monitor of the computer and the observer can save the actual data by mouse click in dedicated .dat files under Windows environment. The data can be imported into the Excel, where the further processing, as multiplication by the correction factors due to the frequency and field strength, etc. is possible.

At low levels the output of the detectors are proportional to the square of the electric field. Therefore the sum of the three signals will be the correct vectorial sum of the square of the total field strength, its square root is the effective value of the field, independent from the polarization.

This calibration is made for each detector individually at each measuring frequency. This calibration function is feed in the Excel program, for computing the corrected value of the field from the output of the detector. In this way the dynamic range can be extended up to 20 dB. The directional sensitivity can be characterised by the ratio of the outputs at parallel and perpendicular polarizations. It is better, than1:100. Fig. 19 shows the probe.